

# Novel kind of decagonal ordering in Al<sub>74</sub>Cr<sub>15</sub>Fe<sub>11</sub>

**Haikun Ma**

University of Science and Technology Beijing

**Zhanbing He** (✉ [hezhanbing@ustb.edu.cn](mailto:hezhanbing@ustb.edu.cn))

State Key Laboratory for Advanced Metals and Materials, University of Science and Technology Beijing

**Hua Li**

University of Science and Technology Beijing

**Tiantian Zhang**

University of Science and Technology Beijing

**Shuang Zhang**

School of Materials Science and Engineering, Dalian Jiaotong University

**Chuang Dong**

Dalian University of Technology

**Walter Steurer**

Department of Materials, ETH Zurich

---

## Article

**Keywords:** Al<sub>74</sub>Cr<sub>15</sub>Fe<sub>11</sub>, Gummelt decagons, Hexagon-Bowtie (HB) tiling, decagonal quasicrystal

**Posted Date:** August 17th, 2020

**DOI:** <https://doi.org/10.21203/rs.3.rs-52725/v1>

**License:** © ⓘ This work is licensed under a Creative Commons Attribution 4.0 International License.

[Read Full License](#)

---

**Version of Record:** A version of this preprint was published at Nature Communications on December 4th, 2020. See the published version at <https://doi.org/10.1038/s41467-020-20077-4>.

# Abstract

A high-angle annular dark field scanning transmission electron microscopy (HAADF-STEM) study of the intermetallic compound  $\text{Al}_{74}\text{Cr}_{15}\text{Fe}_{11}$  reveals a novel kind of aperiodic order. In contrast to the common quasi-unit-cells based on Gummelt decagons, the present structure is related to a covering formed by Andritz decagons, which can also be described by a Hexagon-Bowtie (HB) tiling. This is the first observation of a decagonal quasicrystal with a structure significantly differing from the ones known so far.

## Background

Quasiperiodic structures can be described geometrically either as decorated tilings or as coverings (for a general review see Ref.1, for instance). While tilings are based on two or more unit-tiles, coverings can cover the plane (space) by partially overlapping copies of a single structural repeat-unit (quasi-unit-cell<sup>2-6</sup>). In the case of decagonal quasicrystals, the so-far most abundant quasi-unit-cell is based on the Gummelt decagon<sup>7-10</sup>. Such a quasi-unit-cell, when decorated with atoms (atomic cluster), is the counterpart to a unit cell of a periodic structure. It allows a more physical description of a quasicrystal structure than the structurally fully-equivalent tiling-based models do<sup>6,11,12</sup>.

In the following, we present a quasiperiodic structure that can be described by a covering based on the Andritz decagon, a novel kind of quasi-unit-cell for a decagonal phase. This fundamental decagonal unit, with a diameter of approximately 2 nm, consists of four subunits, three flattened hexagons and one bow-tie ( $\text{D}_{3\text{H}+1\text{BT}}$ , for short).

A decagonal quasicrystal (DQC) with a composition of  $\text{Al}_{74}\text{Cr}_{15}\text{Fe}_{11}$  was identified by transmission electron microscopy (TEM). Figure 1 shows selected-area electron diffraction (SAED) patterns of  $\text{Al}_{74}\text{Cr}_{15}\text{Fe}_{11}$  along the tenfold zone axis (a) and along two typical twofold zone axes perpendicular to it (b, c). Some characteristic features of the diffraction pattern of a DQC, such as its scaling symmetry, are visualized by pentagons of varying size in Fig. 1(a). Note that the spots marked by yellow circles in the SAED pattern are much weaker than the other spots of the largest pentagon, analogously to that of Al-Cr-Fe-Si DQC<sup>5</sup>, but quite different from other typical Al-based DQC systems such as Al-Ni-Co<sup>13,14</sup>, where only strong diffraction spots are found in the corresponding positions. The translation period of the  $\text{Al}_{74}\text{Cr}_{15}\text{Fe}_{11}$  DQC, determined from the two twofold SAED patterns, is  $\approx 1.23$  nm, comparable to that of decagonal Al-Mn-Pd<sup>15</sup>. Consequently, the structure has a translation period of six quasiperiodic atomic layers along the periodic tenfold axis. Every other reciprocal lattice layer is systematically extinct in Fig. 1(c) indicating the existence of a *c*-glide plane. Thus, the 5D symmetry group of this DQC should be  $P10_5/mmc$  like for decagonal Al-Mn-Pd<sup>15</sup>.

The high-angle annular dark field scanning transmission electron microscopy (HAADF-STEM) image, which corresponds to a projection of the structure along the tenfold direction, is depicted in Figs. 2(a, b).

One should keep in mind that such a projection turns the higher-dimensional  $10_5$  screw axis into a simple 10 rotation axis and the  $c$  glide plane into a  $m$  mirror plane, but still in higher dimensions.

Connecting related dots of the image yields a Hexagon-Bowtie (HB) tiling (Fig. 2a). This tiling can be described by a covering as well (Fig. 2b). The covering cluster is a decagon of approximately 2 nm diameter, partitioned by three flattened hexagon tiles and one bowtie tile, called Andritz decagon ( $D_{3H+1BT}$ , for short). An example for a covering created by copies of the Andritz decagon is shown in the tilings encyclopedia<sup>16</sup>. The underlying HB tiling is a substitutional tiling, which scales by even powers of  $\tau$ . Similar as the Gummelt covering it also features an underlying Fibonacci pentagrid (see Fig. 2d).

The  $D_{3H+1BT}$  decagons are superposed onto the HAADF-STEM image in Fig. 2(a) and are filled in light-blue for clear display in Fig. 2(b). Note that the vertices of the  $D_{3H+1BT}$  decagons are themselves decorated with smaller decagons (see also Fig. 3b), but not all are exactly the same. For the vertices of  $D_{3H+1BT}$  to jointly form the thin waist of nearby bowtie (BT) tile, their atomic decorations are not the same as that of the other vertices decorated with the smaller decagons. Nearby  $D_{3H+1BT}$  tiles are connected through both tiling and one "H" covering, to fill some small areas without gaps, but with some gaps for the whole plane, as marked by purple BT and S (star) tiles. These gaps could be considered as defects of quasiperiodic package by the quasi-unit-cell, analogous to the line defects of traditional crystals, for example dislocations. The percentage of area of gaps is 6.1% among the whole filled areas in Fig. 2(b) and can be totally eliminated through the action of phason flipping, for example those in Fig. 2(c) and SFig. 1 in the supporting material.

The purple BT gap in the left column of Fig. 2c-1 is eliminated by being included in a quasi-unit-cell of  $D_{3H+1BT}$  decagon (outlined red) in the right column, after the change of  $H_1$  tile in the left column to the  $H_1'$  tile in the right column. Actually, the change from  $H_1$  to  $H_1'$  tile is simply realized through the phason flipping by changing only one vertex (namely, from black spot to the red spot, as marked by a red arrow in the middle), which was observed experimentally through *in situ* high resolution TEM observations<sup>17,18</sup>. Consequently, the defect of purple BT in the left column is mended and one more quasi-unit-cell is accordingly added, as shown by the red  $D_{3H+1BT}$  in the right column. Sometimes, the phason flipping is somewhat more complex than that in Fig. 2c-1. For example, in order to eliminate defect of purple BT in Fig. 2c-2 in the left column and to also maintain the quasiperiodic repeating of the nearby quasi-unit-cell of  $D_{3H+1BT}$  tiles without gaps, the change of two vertexes of tiles is needed, and resulting in the change of  $H_1$  and  $H_2$  tile in the left column to the  $H_1'$  and  $H_2'$  tile in the right column. Occasionally, the change of three atomic positions is needed (see in SFig. 1a in the supporting materials). For the defect of S tiles in Fig. 2c-3 in the left column, two atomic positions are changed and create two more  $D_{3H+1BT}$  tiles (also see another example in SFig. 1b in the supporting materials), rather than one more  $D_{3H+1BT}$  tile for eliminating BT-type defects mentioned above.

Figure 2d is an idealized quasiperiodic covering based on  $D_{3H+1BT}$  decagons without gaps, derived from Fig. 2b. The gaps of purple BT and S tiles patched in the quasi-unit-cell matrix in Fig. 2b are eliminated

through the action of phason flipping discussed above.

The different allowed arrangements of Gummelt decagons in a strictly quasiperiodic covering (Penrose tiling) are compared to the experimentally observed ones of the Andritz decagons in Fig. 3(a). The Andritz decagon ( $D_{3H+1BT}$ ) in Fig. 3b is generated by linking the centers of the ten smaller rings of white dots (with a diameter of  $\sim 0.47$  nm) with tenfold symmetry. Four more of these small rings located inside the  $\approx 2$  nm decagon, form the three shuttle-like H tiles and one BT tile with an edge length of  $\approx 0.62$  nm. Therefore, the  $D_{3H+1BT}$  has just mirror symmetry, similar to the Gummelt's decagon. However, while the reflection plane runs through corners in the case of the Gummelt decagon, it is perpendicular to decagon edges in the case of the Andritz decagon.

In contrast, the  $D_{3H+1BT}$  are linked to their neighbors by either overlapping H tiles or sharing one edge (Fig. 3b). The distance between the centers of adjacent  $D_{3H+1BT}$  decagons with overlapping H tiles amounts to  $S = 1.18$  nm, and to  $L = \tau S = 1.91$  nm when the  $D_{3H+1BT}$  decagons are sharing edges. For the linkage of more  $D_{3H+1BT}$  decagons, for example three, four, five and more  $D_{3H+1BT}$  tiles see SFig. 2 in the Supporting materials. The simple connection rules in Fig. 3(b) allow to cover the whole plane without gaps, implying the  $D_{3H+1BT}$  can act as a repeating quasi-unit-cell generating a quasiperiodic long-distance order<sup>16</sup>.

We now analyze the local features and the long-distance quasiperiodic ordering of the quasi-unit-cell of  $D_{3H+1BT}$  tiles in Fig. 2d by linking their centers with solid green lines in Fig. 4a. The somewhat disordered quasiperiodic tiling superimposed on Fig. 2d is formed by linking the centers of two nearby  $D_{3H+1BT}$  tiles covered by one H tile, with a 1.18 nm edge length of tiles. The structural blocks include regular pentagon (P), large decagon with a tangential circle diameter of 3.63 nm, as well some irregular shapes such fat hexagon ( $H_F$ ), banana-like tile (BLT), and concave decagon ( $D_C$ ). Among them, 19 pentagons are found, with the positions one-to-one corresponding to the 19 groups of five H tiles with a fivefold symmetry in Fig. 2d, for example one position marked by one red star in the upper-left corner in Fig. 4a. Irregular polygons were mostly found in imperfect DQCs<sup>19-22</sup>, implying the quasiperiodic ordering in Fig. 4a is not perfect. Interestingly, we find that some of  $D_{3H+1BT}$  decagons (for example those highlighted in thick blue edges) tend to locate locally at the vertexes of a larger decagon with a tangential circle diameter of 5.88 nm, as those marked by dotted purple decagons. These  $D_{3H+1BT}$  tiles share one edge with neighbors and distribute according to tenfold symmetry around one center of  $D_{3H+1BT}$  tile, analogous to the experimental tenfold symmetric distribution of  $\approx 2$  nm decagons in decagonal  $Al_{59}Cr_{21}Fe_{10}Si_{10}$ <sup>23</sup>. Furthermore, we note that there are 116 decagons in Fig. 4a distributed along 10 directions differing  $36^\circ$ . Fig. 4b schematically show the directions of decagons, where the BT tile in each decagon is filled by colors to guide the eye for the orientations of decagons. Among them, every two of  $180^\circ$  oriented decagons are in a pair and colored in the same. We count the decagons along each direction and summarized in the histogram in Fig. 4c, where the maximum, minimum, and averaged number of decagons is 16, 8 and  $11.1 \pm 2.1$ , respectively. The difference of the counts of decagons along each direction also implies the imperfect quasiperiodic tiling.

The finding of a quasi-unit-cell different from those based on the Gummelt decagon shows that quasiperiodic order is possible based on a variety of fundamental structural subunits. But both, the Gummelt as well as the Andritz covering have in common that their structural subunits are arranged along quasi-lattice planes with traces forming Fibonacci pentagrids. These planes may be important for the evolution of quasiperiodic long-range order (see Refs.24,25).

## Methods

Approximately 1 Kg of the master Al-Cr-Fe alloy with a nominal composition of  $\text{Al}_{72}\text{Cr}_{16}\text{Fe}_{12}$  was prepared by melting high-purity elements in an induction furnace under vacuum. Several small pieces of sample from the cast ingot of the alloy were heated at 1025°C for 7 days in an evacuated quartz tube, and then cooled in the furnace by shutting off the power. Part of the sample after the heat treatment was then annealed at 1000°C for 7 days in a vacuum, and then quenched in the water.

Powder samples were adapted for transmission electron microscopy (TEM) observations. A FEI Tecnai F30 transmission electron microscope equipped with an energy dispersive X-ray spectrometer (EDS) was first used to check the phases and the composition. A JEM-ARM200F transmission electron microscope equipped with a Cs-probe corrector and Cs-image corrector was used to obtain high-angle annular dark field scanning transmission electron microscopy (HAADF-STEM) images at an atomic resolution. The inner and outer acceptance semi-angles for HAADF-STEM imaging were 90 and 370 mrad, respectively.

## Declarations

## Author contributions

Z.H. conceived the research; H.M. performed the experiments; Z.H., H.M., W.S. wrote the manuscript. All authors analysed the data, discussed the results, and drew the conclusions.

## Competing interests

The authors declare no competing interests.

## Acknowledgments

This work was supported by the National Natural Science Foundation of China (51871015 and 51471024). We thank Mr Xinan Yang of the Beijing National Laboratory for Condensed Matter Physics, Institute of Physics, Chinese Academy of Sciences for assistance in recording the HAADF-STEM images.

## References

1. Steurer, W. Quasicrystals: What do we know? What do we want to know? What can we know? *Acta Cryst. A* **74**, 1–11 (2018).
2. Steinhardt, P. J. et al. Experimental verification of the quasi-unit-cell model of quasicrystal structure. *Nature* **396**, 55–57 (1998).
3. Steinhardt, P. J. & Jeong, H. C. A simpler approach to Penrose tiling with implications for quasicrystal formation. *Nature* **382**, 431–433 (1996).
4. Abe, E. et al. Quasi-unit-cell model for an Al-Ni-Co ideal quasicrystal based on clusters with broken tenfold symmetry. *Phys. Rev. Lett.* **84**, 4609–4612 (2000).
5. He, Z. B., Ma, H. K., Li, H., Li, X. Z. & Ma, X. L. New type of Al-based decagonal quasicrystal in Al<sub>60</sub>Cr<sub>20</sub>Fe<sub>10</sub>Si<sub>10</sub> alloy. *Sci. Rep.* **6**, 22337 (2016).
6. Deloudi, S., Fleischer, F. & Steurer, W. Unifying cluster-based structure models of decagonal Al-Co-Ni, Al-Co-Cu and Al-Fe-Ni. *Acta Cryst. B* **67**, 1–17 (2011).
7. Gummelt, P. Penrose tilings as coverings of congruent decagons, *Geom. Dedicata* **62**, 1–17 (1996).
8. Gummelt, P. & Bandt, C. A cluster approach to random Penrose tilings, *Mater. Sci. Eng.* **294–296**, 250–253 (2000).
9. Gummelt, P. Random cluster covering model, *J. Non-Cryst. Solids* **334&335**, 62–67 (2004).
10. Reichert, M. & Gähler, F. Cluster model of decagonal tilings, *Phys. Rev. B* **68**, 214202 (2003).
11. Steurer, W. Stable clusters in quasicrystals: fact or fiction? *Philos. Mag.* **86**, 1105–1113 (2006).
12. Steurer, W. Twenty years of structure research on quasicrystals. Part I. Pentagonal, octagonal, decagonal and dodecagonal quasicrystals. *Z. Kristallogr.* **219**, 391–446 (2004).
13. Tsai, A.P., Fujiwara, A., Inoue, A. & Masumoto, T. Structural variation and phase transformations of decagonal quasicrystals in the Al-Ni-Co system. *Phil. Mag. Lett.* **74**, 233–240 (1996).
14. Ritsch, S. et al. Highly perfect decagonal Al-Co-Ni quasicrystals. *Phil. Mag. Lett.* **74**, 99–106 (1996).
15. Steurer, W., Haibach, T., Zhang, B., Beeli, C. & Nissen, H.U. The Structure of Decagonal Al<sub>70.5</sub>Mn<sub>16.5</sub>Pd<sub>13</sub>. *J. Phys. Cond. Matter* **6**, 613–632 (1994).
16. Frettlöh, D., Harriss, E. & Gähler, F. Tilings encyclopedia, <https://tilings.math.uni-bielefeld.de/substitution/bowtie-hexagon/>
17. Edagawa, K., Suzuki, K. & Takeuchi, S. High resolution transmission electron microscopy observation of thermally fluctuating phasons in decagonal Al-Cu-Co. *Phys. Rev. Lett.* **85**, 1674–1677 (2000).
18. Edagawa, K., Suzuki, K. & Takeuchi, S. HRTEM observation of phason flips in Al-Cu-Co decagonal quasicrystal. *J. Alloys Compd.* **342**, 271–277 (2002).
19. Hiraga, K. & Yasuhara, A. Arrangements of transition-metal atoms in three types of AlCoNi Decagonal Quasicrystals Studied by Cs-Corrected HAADF-STEM. *Mater. Trans.* **54**, 493–497 (2013).
20. Sun, W., Ohsuna, & T. Hiraga, K. Structural characteristics of a high-quality Al-Ni-Ru decagonal quasicrystal with 1.6 nm periodicity, studied by atomic-scale electron microscopy observations. *Phil. Mag. Lett.* **81**, 425–431 (2001).

21. Hiraga, K., Sun, W., Lincoln, F. J., Kaneko, & M. Matsuo, Y. Formation of decagonal quasicrystal in the Al-Pd-Mn system and its structure. *Jpn. J. Appl. Phys.* **30**, 2028–2034 (1991).
22. Hiraga, K. & Sun, W. Tiling in Al-Pd-Mn decagonal quasicrystal, studied by high-resolution electron microscopy. *J. Phys. Jpn.* **62**, 1833–1836 (1993).
23. Ma, H. K., He, Z. B. Hou, L. G. & Steurer, W. Exceptionally large areas of local tenfold symmetry in decagonal  $\text{Al}_{59}\text{Cr}_{21}\text{Fe}_{10}\text{Si}_{10}$ . *J. Alloys Compd.* **765**, 753–756 (2018).
24. Kuczera, P. & Steurer, W. Cluster-based growth algorithm for decagonal quasicrystals. *Phys. Rev. Lett.* **115**, 085502 (2015).
25. Steurer, W. & Cervellino, A. Quasiperiodicity in decagonal phases forced by inclined net planes? *Acta Crystallogr. A* **57**, 333–340 (2001).

## Figures

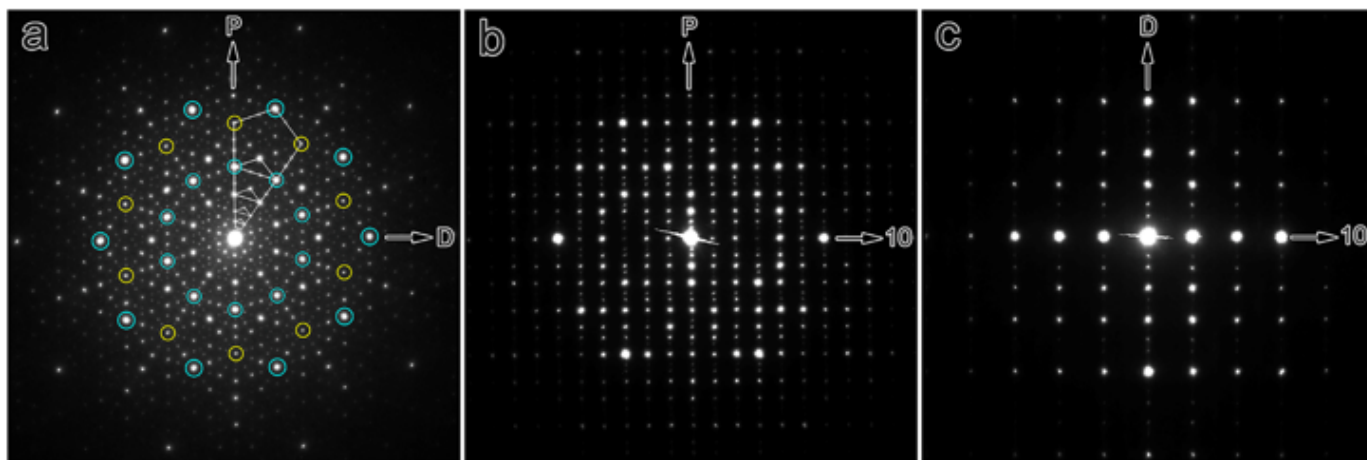


**Figure 1**

SAED patterns of  $\text{Al}_{74}\text{Cr}_{15}\text{Fe}_{11}$ . a, Taken along the tenfold axis and b, c, along two typical twofold zone axes normal to that in a. Some features are marked in a demonstrating the scaling properties of the diffraction pattern by powers of  $\tau = 1.618$ . Every other reciprocal lattice layer is systematically extinct in c, indicating the existence of a c-glide plane.

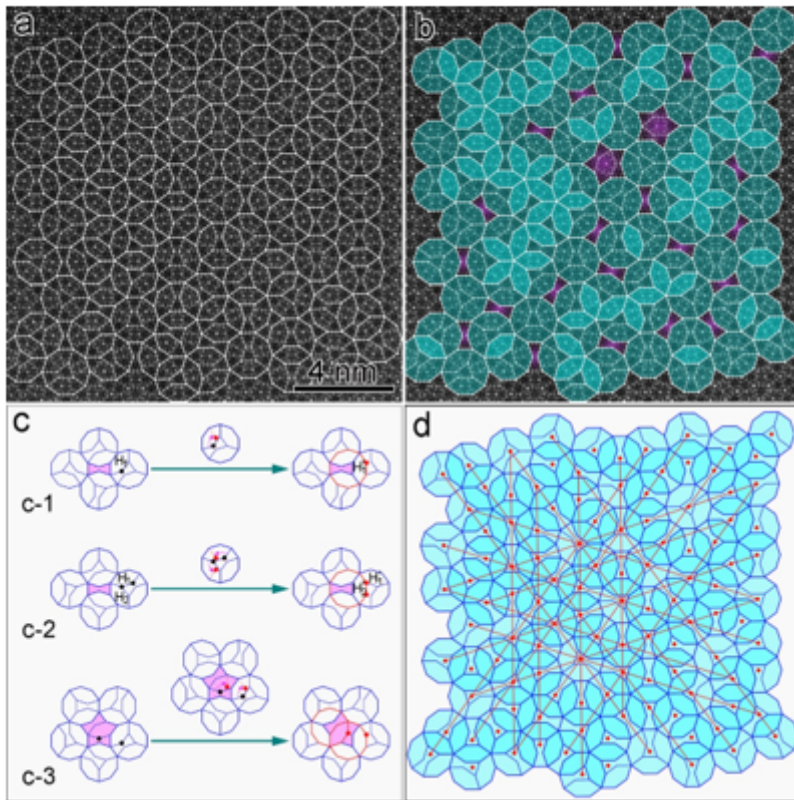


**Figure 2**

Quasiperiodic tiling of the quasi-unit-cell of D3H+1BT. a, HAADF-STEM image along the tenfold axis of Al<sub>74</sub>Cr<sub>15</sub>Fe<sub>11</sub> DQC with the quasi-unit-cell of D3H+1BT superposed. b, The quasi-unit-cell of D3H+1BT is filled in blue to clearly show the structural tiling. The 93.9% area of the whole filled areas is covered by the quasi-unit-cell of D3H+1BT, and only 6.1% is uncovered, as marked in purple. c, The action of phason flipping to eliminate the defects (namely the purple area) in b. One or two more 2.0 nm decagons are generated in the right column with the disappearance of purple defects in the left column. d, One quasiperiodic tiling reproduced from b is forced using the single quasi-unit-cell of D3H+1BT tile. The centers of D3H+1BT tiles are marked by red dots.

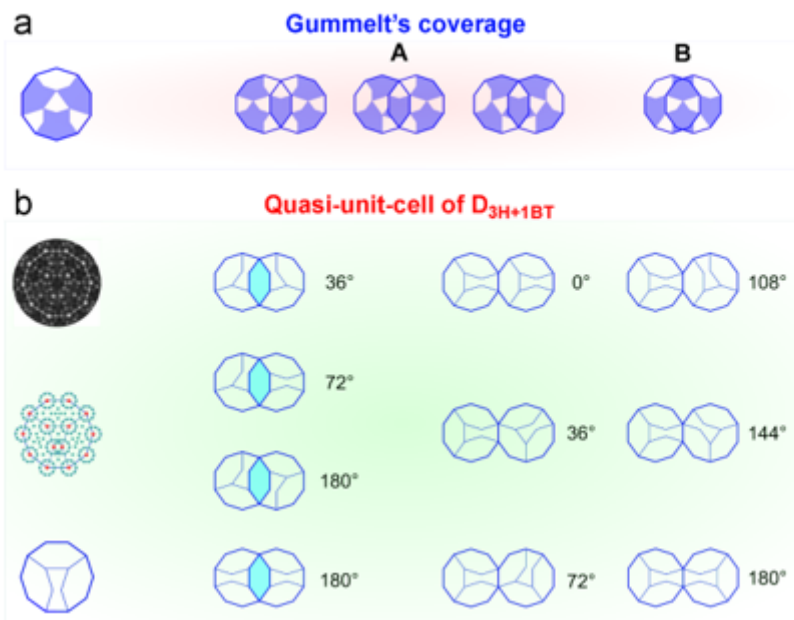


**Figure 3**

Comparison of Gummelt decagons and the experimentally observed quasi-unit-cell of  $D_{3H+1BT}$ . a, Allowed arrangements of Gummelt decagons. Middle and right: A- and B-type coverage with strict matching rules (refer to [7] for details). b, Quasi-unit-cell of  $D_{3H+1BT}$  in this paper. Left column: experimental image, projected structural model (Red atoms: Cr/Fe; blue atoms: Al) and schematic diagram of the quasi-unit-cell of  $D_{3H+1BT}$  with a circumscribed circle diameter of 2.0 nm. Middle and right: typical connections of nearby  $D_{3H+1BT}$  tiles through overlapping an H tile or sharing one edge in to produce two distances of the decagon centers:  $S = 1.18$  nm, and  $L = \sqrt{3} S = 1.91$  nm. Their connections are relatively simple without strict matching rules. The orientations of nearby decagons are differed by several angles, as shown aside.

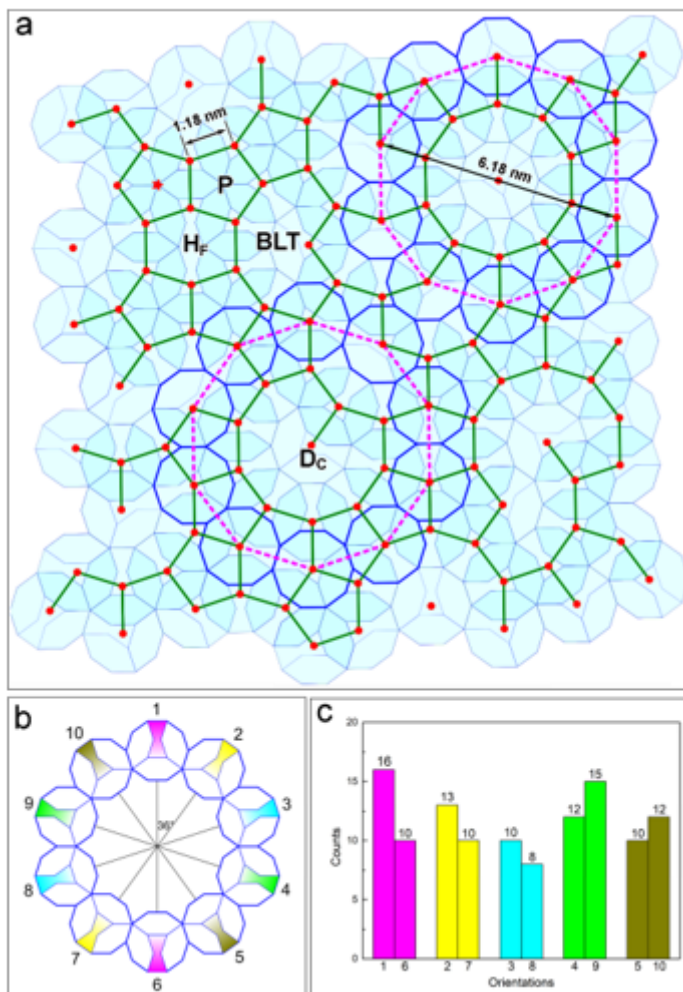


**Figure 4**

Random quasiperiodic tiling superimposed on Fig. 2d by linking the centers of nearby overlapping D3H+1BT tiles. a, Note larger decagons with a circumscribed circle diameter of 6.18 nm (tangential circle diameter of 5.88 nm), as those marked by dotted purple decagons, can be generated by linking the centers of some 2.0 nm decagons sharing edges. b, Ten orientations of D3H+1BT tiles differing 36° in a. c, Corresponding histogram of counts of decagons along each orientation. The average count of decagons along each direction is 11.1 ± 2.1.

## Supplementary Files

This is a list of supplementary files associated with this preprint. Click to download.

- [FigS1.png](#)
- [FigS2.png](#)